SYNTHESIS AND CHARACTERIZATION OF GOAT BONE-DERIVED HYDROXYAPATITE - ZINC OXIDE NANOCOMPOSITES FOR BIOMEDICAL APPLICATION

Lin Lin Naing[1], Ni Ni Sein[2], Thida Win[3]

Abstract

Hydroxyapatite (HAp) obtained from the chemical treatment (HCl and NaOH) and calcination at 900 ºC of fresh goat bone were incorporated with different amounts of zinc oxide (ZnO) nanoparticles (5 % and 10 %) to give HAp-ZnO nanocomposites (20:1 and 20:2). These nanocomposites were indexed as hexagonal structure with equal length of a and b but shorter c. FT IR spectral data revealed the characteristic absorption peaks of PO_4^{3-}, OH^- and ZnO in HAp-ZnO nanocomposites. SEM images of HAp-ZnO nanocomposites were elongated crystalline structures with agglomeration of ZnO on the surface of HAp. The bulk density of the nanocomposites slightly increased and the porosity percentage decreased as the temperature and amount of zinc oxide increased. HAp and HAp-ZnO nanocomposites (20:1 and 20:2) prepared at 1000 ^oC showed no cytotoxic effect tested by brine shrimp assay. Orthopedic applications of HAp and HAp-ZnO nanocomposites were conducted by using Wistar rats. By X-ray diagnosis HAp-ZnO composites exhibited as a promising filler of bone defect. Histological findings showed that HAp-ZnO composites with ratio of 20:2 at 1000 °C group was found to be the best with the good scoring within 30 days after application.

Keywords: Goat bone, hydroxyapatite, zinc oxide, nanocomposites, brine shrimp assay, orthopedic applications

Introduction

Bone is a highly specialized supporting frame-work of the body (Kini and Nandeesh, 2012). It comprises of organic and inorganic fractions being in continuous interchange with each other for bone-forming and resorbing. The main part of the hard inorganic structure of the bone is hydroxyapatite [$Ca_{10}(PO_4)_6(OH)_2$]. Hydroxyapatite (HAp) is chemically identical to the inorganic matrix of living bones (Ylinen, 2006). HAp exhibits excellent

[1.] Dr, Assistant Lecturer, Department of Chemistry, Mandalar Degree College
[2.] Dr, Professor (Retired), Department of Chemistry, University of Yangon
[3.] Dr, Rector, University of Mandalay

biocompatibility both with hard tissue and with soft tissue (Okada and Matsumoto, 2015; Zhou and Lee, 2011).

Currently, metals are widely used in orthopedics to increase the bioactivity of hydroxyapatite. Among these metals, zinc is an essential trace element present in human bones and teeth. It plays important roles in increasing osteoblast adhesion and alkaline phosphatase activity of bone cells (Deepa *et al*., 2013). Zinc oxide (ZnO) creates much attention as a future material because it can be used as a versatile material for immense applications (Zak *et al*., 2013). Zinc oxide is a white inorganic compound and insoluble in water. ZnO is a key technological material (Singh *et al*, 2012). It is a bio-safe and biocompatible material and can be directly used for biomedical applications without coating (Anita *et al*, 2010).

Hydroxyapatite with various additives like ZnO and MgO were mainly prepared to obtain superior quality materials suitable for use in artificial bone substitution. Properties of HAp such as morphology, crystallinity and crystal size distribution have great influence in the production of materials for biomedical applications. Therefore, it is essential to optimize how these properties of HAp are affected by different additives (Deepa *et al*, 2013).

The aim of the present study is to synthesize and characterize goat bone-derived hydroxyapatite and zinc oxide nanocomposites and to study the biomedical application of the prepared nanocomposites.

Materials and Methods

Sample Collection

The raw goat bone samples were directly collected from retail market in Mandalay Region.

Preparation of Hydroxyapatite from Waste Goat Bone

The goat bones were firstly cleaned with water to remove dirty substances and then boiled in a pot at 100 ˚ C for several hours to get rid of any remaining unwanted materials. The bones (500 g) were initially deproteinized through external washing with 1 L of 1 M hydrochloric acid solution for 24 h at room temperature. Next, the deproteinized goat bones

were thoroughly washed several times with distilled water. After that, the bones were treated with 1 L of 1 M sodium hydroxide solution for 24 h to remove the remaining proteins of goat bones. After filtration, the goat bones were thoroughly washed with distilled water again and again and then dried at 60 ° C in hot air oven for several hours. The dried bones were crushed into small chips and transformed to fine powder using a mortar and pestle. Finally, a yellowish white hydroxyapatite powder was obtained. Then it was calcined at 900 ^{o}C in a muffle furnace (DFM-05, Korea) for 3 h. The calcined powder samples were cooled and then stored in a desiccator for further studies.

Preparation of Zinc Oxide Nanoparticles

ZnO nanoparticles were prepared by wet chemical method (Nawaz *et al*., 2011). The precursors used in the preparation of ZnO were zinc nitrate hexahydrate and sodium hydroxide. Soluble starch as stabilizer was also used in the preparation of zinc oxide sample (Yadav *et al*., 2006). Initially, 100 mL of 0.1 % starch solution was prepared in distilled water. Then, 0.4 mol of zinc nitrate was added to 0.1 % starch solution. To achieve complete dissolution of zinc nitrate, the solution obtained was mixed using a magnetic stirrer under constant stirring. After that, 0.8 mol of sodium hydroxide solution was poured drop-wise along the side walls of the above mixture solution vessel under continuous stirring. After complete addition of sodium hydroxide, the mixture was continued to stir for 2 h. When the reaction was complete, the solution was kept overnight. The supernatant liquid was carefully decanted and the remaining solution was centrifuged at 4500 rpm for 10 min. Moreover, to remove the by-products and any starch bound to the sample, the resulting sample was washed 2-3 times with ethanol-water using centrifugal apparatus. The final step was to dry the sample in an oven at 80 °C for 3 h and to anneal in a muffle furnace at 400 °C for 3 h for conversion of $Zn(OH)_2$ to ZnO.

Preparation of HAp-ZnO Nanocomposites

The solution of ZnO (25 % w/v in distilled water) was prepared with the aid of a magnetic stirrer for 1 h. The HAp solution was also prepared using the ratio of 1:1 for powder (g) and water (mL) by means of magnetic stirring

for 1 h to get homogeneity of the dispersion. In order to prepare HAp-ZnO nanocomposites, the weight percentages (wt %) of ZnO were chosen as 5 and 10. The prepared ZnO solution was poured into the HAp solution and then thoroughly mixed using stirrer at 80-90 °C for 1 h. The obtained suspension was cooled to room temperature for 12 h. In addition, it was filtered using a funnel through filter paper. The residues were washed 2 to 3 times with distilled water. Then, it was transferred into porcelain basin and placed in an oven at 120 °C for 4 h to obtain dried sample. Moreover, the resulting products were calcined at 600 °C, 800 °C and 1000 °C for 2 h.

Characterization Techniques

The phase purity was examined by using Rigaku X-ray diffractometer (Rigaku Co., Japan) with Cu Kα (λ =1.54056 Å) radiation over a range of 2θ angles from 10° to 70°. Various functional groups present in the prepared HAp-ZnO composites calcined at different temperatures were identified by FT IR (Perkin Elmer). The scanning electron microscope (SEM, JEOL-JSM-5610 LV, Japan) was used for the morphological study of HAp-ZnO composites. Relative abundances of elements in HAp-ZnO composites were qualitatively determined by EDXRF analysis using EDX-702 spectrometer (Shimadzu Co. Ltd., Japan) at Universities' Research Center, Yangon.

Physical Properties of HAp and HAp-ZnO Nanocomposites

pH was determined by pH meter, and bulk density and porosity of the samples were determined by tapping method and liquid displacement method respectively.

Cytotoxicity Assay

The brine shrimp *(Artemia salina*) was used in this study for cytotoxicity bioassay. Brine shrimp cysts (0.5 g) were added to the 1.5 L of artificial sea water bottle. Artificial sea water was prepared by dissolving 26.518 g of sodium chloride, 2.447 g of magnesium chloride, 3.305 g of magnesium sulphate, 1.141 g of calcium chloride, 0.725 g of potassium chloride, 0.202 g of sodium hydrogen carbonate and 0.083 g of sodium bromide in distilled water in a 1 L volumetric flask and the volume made up

to the mark with distilled water (Sverdrup *et al*., 1942). The bottle containing the brine shrimp was placed near a lamp. Light is essential for the cysts to hatch. Brine shrimp cysts required to hatch constant supply of oxygen for 24 h incubation at room temperature.

Artificial sea water (9 mL) and 1 mL of each of HAp, different concentrations of HAp-ZnO composites with the weight ratios of 20:1 and 20:2 (0.1, 1, 10, 100 and 1000 µg/mL) and standard potassium dichromate solutions were added to each chamber. Alive brine shrimp (10 nauplii) were then taken with pasture pipette and placed into each chamber. After incubation at room temperature for about 24 h, the number of dead brine shrimps was counted and 50 % lethality dose (LD_{50}) was calculated. The control solution was prepared as the above procedure by using distilled water instead of sample solution.

Biomedical Application of Hydroxyapatite-Zinc Oxide Nanocomposites by Animal Experiment (*in vivo* Test)

Eight healthy Wistar rats (male with 250-300 g body weight) were chosen for this experiment. Rats were provided by Laboratory Animal Service Division, Department of Medical Research, Yangon. Animals were kept individually in standard rat cages with an ambient temperature of 24 ºC and 12/12 light/dark cycle. The animals had free access to drinking water and standard laboratory pellets.

Animals were divided into four individual groups in this experiment. For Group I, skull defect was filled with HAp calcined at 900 ^{o}C after surgery procedure. For Group II, the skull defect was filled with HAp-ZnO (20:1) calcined at 1000 ^{o}C and for Group III it was filled with HAp-ZnO (20:2) calcined at 1000 ^{o}C. However, skull defect was not filled any composites materials for Group IV.

All animals used for surgical performance in this study received general anesthesia via an intramuscular injection with 0.5 mL Ketamine associated with 0.1 mL Xylazine. The hair of each rat skull was firstly shaved and the area was cleaned before operation. After shaving the area, a linear skin incision was made in the dorsal portion of skull bone of each rat with surgical knife. Then, the skull bone area was created the identical bony defect

well of such animal using stainless hand drill under anaesthetized condition. The nanocomposite powder was taken in a watch glass and distilled water added dropwise till the powder got fully wet and then stirred to become paste. The paste was molded in the skull bone cavity before suturing. Defects were gently packed with HAp at 900 °C paste for Group (I) animal, HAp-ZnO nanocomposite (20:1) at 1000 °C paste for Group (II) animal, HAp-ZnO nanocomposite (20:2) at 1000 °C for Group (III) and other defect was left unfilled, i.e., control for Group (IV) animal.

After obtaining adequate hemostasis, the flap (skin layer) was closed with suturing cat gut continuously after the operation procedures and dressed with betadine solution for the superfacial wound healing. After surgery, animals were kept in separate cages and were fed with pellet food made in DMR and clean water *ad libitum*. All animals showed good general health condition throughout the study as assessed by their weight gain.

Radiologic examination of skull bone defects progression was carried out at 14 days and 30 days after surgery at Crown Veterinary Resources. For histological analysis the samples were fixed in a 10 % phosphate-buffer formaldehyde solution for at least 3 days. The stained sections of each test sample were examined using light microscopy for tissue inflammatory reaction and the presence of the characteristic features of bone formation and cellular reaction to the implanted materials.

Results and Discussion

X-Ray Diffraction (XRD) Analysis of Prepared HAp, ZnO and HAp-ZnO Nanocomposites

Sharp and narrow peaks of HAp with high intensity of crystalline patterns were observed in the XRD spectrum of HAp calcined at 900 ^{o}C (Figure 1a). The well-defined peaks of ZnO observed in XRD spectrum of ZnO calcined at 400 ^{o}C (Figure 1b) are in agreement with the library data of ZnO. In comparison with the standard ZnO, no other diffraction peaks were detected which proved that the prepared ZnO is pure.

Figure 2 shows XRD patterns of HAp-ZnO nanocomposites with weight ratios of 20:1 and 20:2 at three different temperatures of 600 ^{o}C,

800 ^{o}C and 1000 ^{o}C. Well-defined peaks of HAp and ZnO were clearly seen. Diffraction peaks of HAp-ZnO nanocomposites revealed that the principal components of HAp and ZnO were well developed in all of these samples. The same observation was reported by Moldovan *et al.* (2015). The principal peaks of HAp appeared at Miller indices of (211), (112), (300), (130), (222) and those of ZnO at (100), (002), (101), (110) and (103).

Table 1 shows the changes in size and crystallinity percentages of HAp-ZnO nanocomposites obtained by two different ratios of 20:1 and 20:2 at 600 ^{o}C, 800 ^{o}C and 1000 ^{o}C. Crystallite sizes of HAp-ZnO (20:1) were 40.28 nm, 41.00 nm and 44.63 nm and those of HAp-ZnO (20:2) were 40.25 nm, 42.01 nm and 49.10 nm for the samples calcined at 600 ^{o}C, 800 ^{o}C and 1000 ^{o}C, respectively. All the crystallite sizes were within the nano range. Crystallite size increased with increase in temperature. Similar changing patterns of crystallinity percentages were observed for HAp-ZnO nanocomposites. Crystallinity percentages were in the range of 61.29 to 67.56 % and 65.79 to 75.20 % for HAp-ZnO nanocomposites (20:1) and (20:2), respectively. Furthermore, changes of lattice constants of HAp derived from goat bone and HAp-ZnO nanocomposites are shown in Table 2. It was observed that lattice constants a, b and c of HAp derived from goat bone changed after incorporation of ZnO.

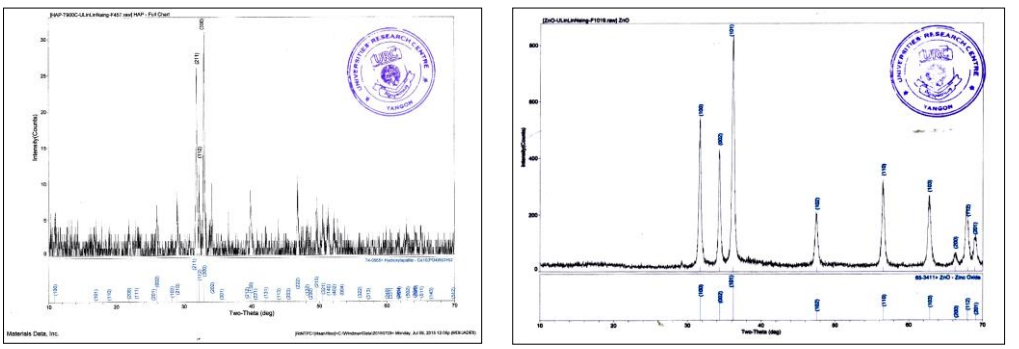

(a) (b)

Figure 1: XRD diffractograms of (a) HAp calcined at 900 °C and (b) ZnO calcined at 400 °C

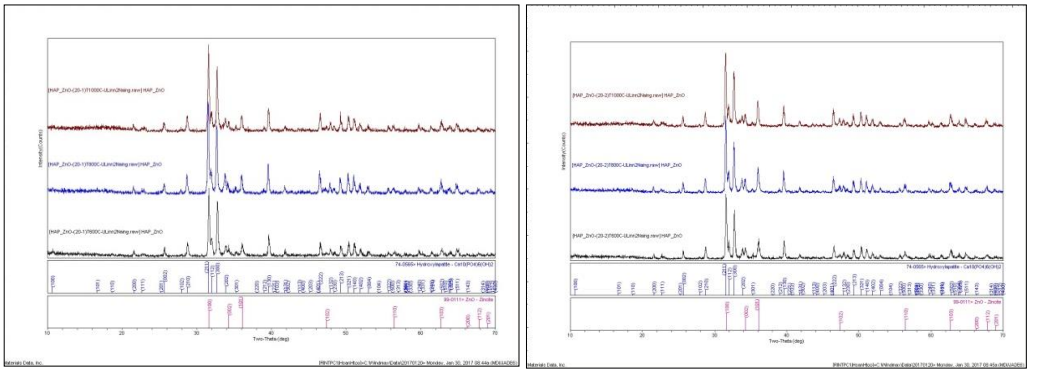

(a) (b)

Figure 2 : Comparison of XRD diffractograms of (a) HAp-ZnO (20:1) at 600 °C, 800 °C and 1000 °C (b) HAp-ZnO (20:2) at 600 ºC, 800 ºC and 1000 ºC

Table 1: Comparison of Average Crystallite Sizes and Percent Crystallinity of HAp, ZnO Nanoparticles and HAp-ZnO Nanocomposites

No	Samples	Average crystallite size (nm)	Percent crystallinity (%)
1	Hydroxyapatite at 900 ºC	81.13	59.35
2	HAp-ZnO (20:1) at 600 ºC	40.28	61.29
3	HAp-ZnO (20:1) at 800 ºC	41.00	65.63
4	HAp-ZnO (20:1) at 1000 ºC	44.63	67.56
5	HAp-ZnO (20:2) at 600 ºC	40.25	65.79
6	HAp-ZnO (20:2) at 800 ºC	42.01	69.82
7	HAp-ZnO (20:2) at 1000 ºC	49.10	75.20
8	ZnO	24.12	

Table 2: Comparison of Lattice Constants of HAp, ZnO Nanoparticles and HAp-ZnO Nanocomposites

Samples	Lattice Constants (Å)			Crystal structure
	a	b	c	
Hydroxyapatite at 900 ºC	9.3893	9.3893	6.8688	Hexagonal
HAp-ZnO (20:1) at 600 ºC	9.4834	9.4834	6.8913	Hexagonal
HAp-ZnO (20:1) at 800 ºC	9.5053	9.5053	6.9494	Hexagonal
HAp-ZnO (20:1) at 1000 ºC	9.4930	9.4930	6.8575	Hexagonal
HAp-ZnO (20:2) at 600 ºC	9.4914	9.4914	6.9104	Hexagonal
HAp-ZnO (20:2) at 800 ºC	9.5146	9.5146	6.9200	Hexagonal
HAp-ZnO (20:2) at 1000 ºC	9.5187	9.5187	6.8548	Hexagonal
Zinc Oxide	3.2580	3.2580	5.2126	Hexagonal

Fourier Transform Infrared (FT IR) Analysis of HAp-ZnO nanocomposites

The FT IR spectra of HAp-ZnO nanocomposites with two different ratios calcined at 600 ^{o}C, 800 ^{o}C and 1000 ^{o}C are illustrated in Figures 3. The main chemical groups that characterize HAp and ZnO structures such as PO_4^{3-}, OH^-, CO_3^{2-} and ZnO were found in the FT IR spectra. From the spectral data, the characteristic absorption bands of zinc oxide were observed in the range of 400-500 cm^{-1} due to stretching mode of Zn-O (Vanaja and Rao, 2016). Absorption peak of ZnO (418 cm^{-1}) shifted to higher wavenumbers in the range of 437 to 474 cm^{-1} in HAp-ZnO nanocomposites. The peaks around 1091 cm^{-1} and 1045 cm^{-1} correspond to the stretching of P-O in phosphate group. The bands observed around 1460 cm^{-1} and 1413 cm^{-1} are attributed to carbonate group (Figueiredo *et al*., 2010). Moreover, O-H stretching vibration of hydroxyl group was observed at 3400-3500 cm^{-1}. There is no apparent change in band positions in HAp-ZnO nanocomposites with different temperatures and various ratios of zinc oxide. However, the band positions of P-O stretching and bending vibrations and O-H stretching vibrations of HAp slightly shifted from their original positions after incorporation of ZnO.

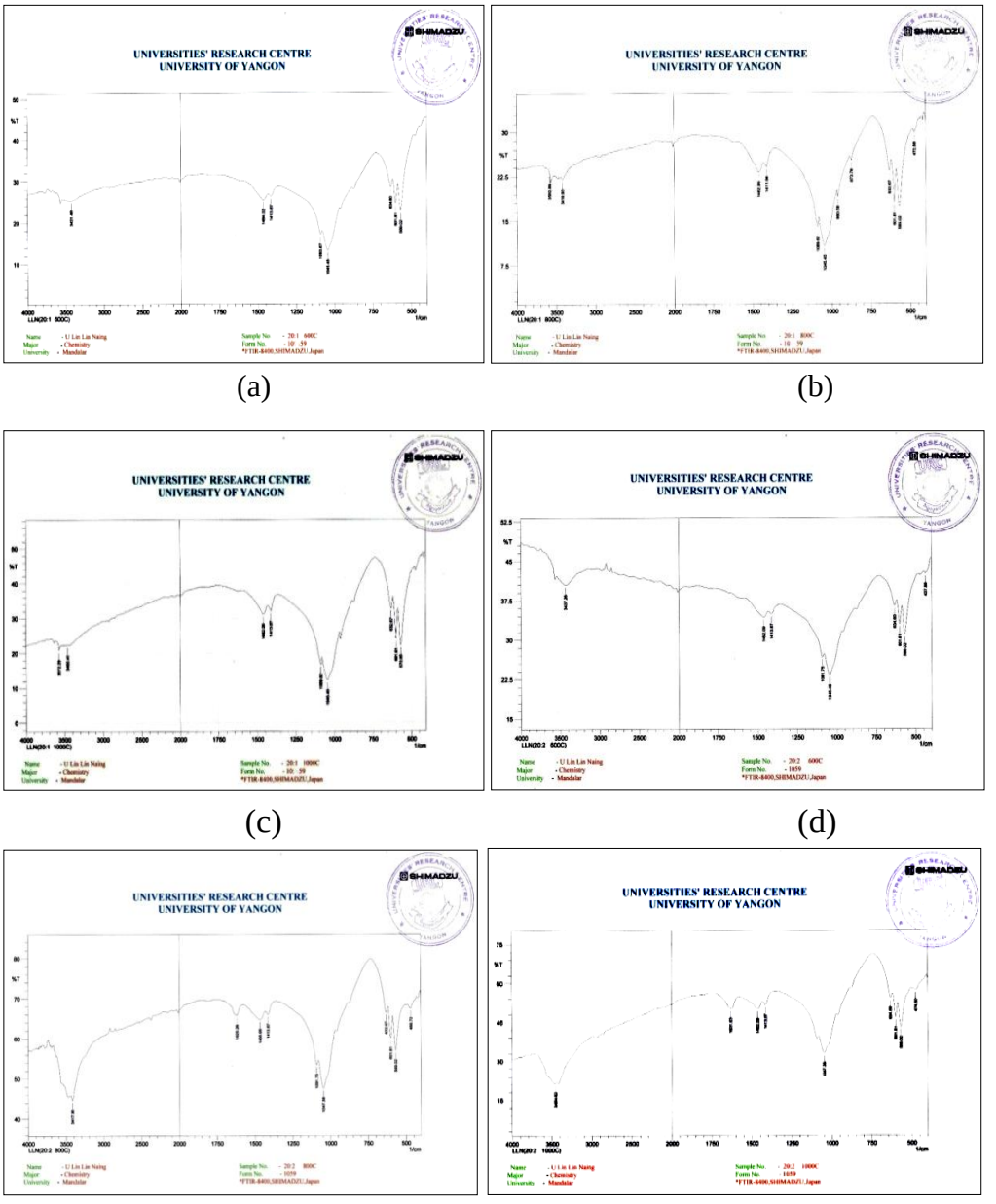

Figure 3: FT IR spectra of HAp-ZnO (20:1) calcined at (a) 600 ºC (b) 800 ºC (c) 1000 ºC and HAp-ZnO (20:2) calcined at (d) 600 ºC (e) 800 ºC and (f) 1000 ºC

Scanning Electron Microscopy (SEM) Analysis of Prepared HAp and HAp-ZnO Nanocomposites

SEM images of HAp-ZnO nanocomposites are depicted in Figure 4. Discrete particles of HAp particles were observed in HAp derived from goat bone calcined at 900 ^{o}C. After incorporation of ZnO to HAp the elongated crystalline forms were observed in all HAp-ZnO nanocomposites. Furthermore, agglomeration of ZnO nanoparticles on the surface of HAp were noted.

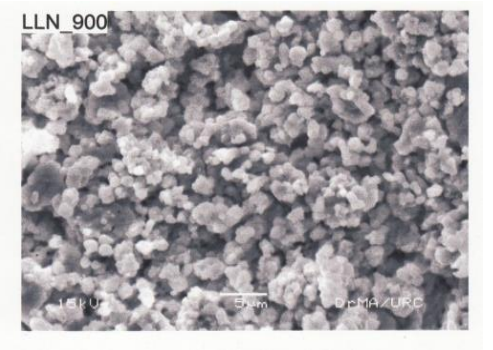

(a)

(b)

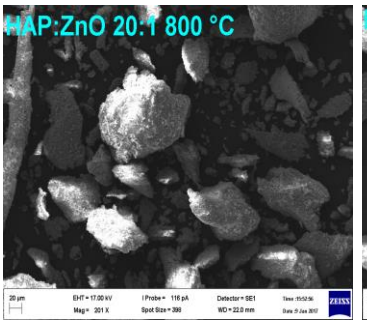

(c)

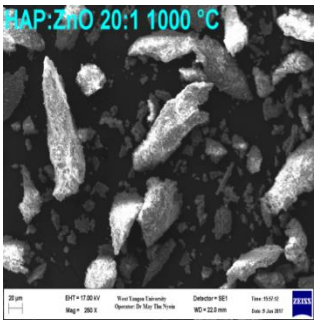

(d)

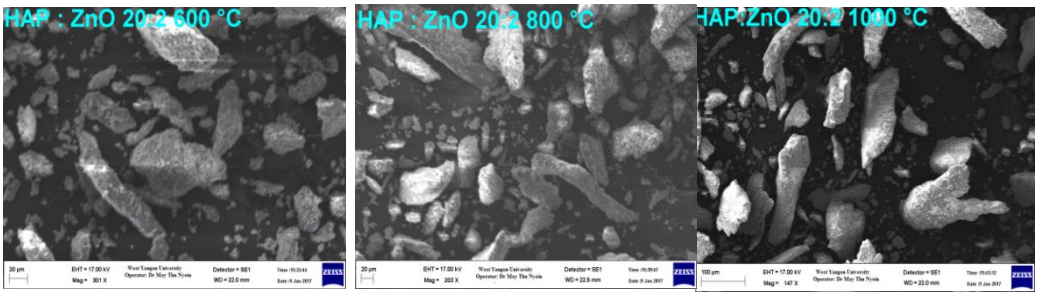

(e) (f) (g)

Figure 4 : SEM images of (a) HAp (900 ^{o}C) (1000X magnification)
(b) HAp-ZnO 20:1 (600 ^{o}C) (242X magnification)
(c) HAp-ZnO 20:1 (800 ^{o}C) (201X magnification)
(d) HAp-ZnO 20:1 (1000 ^{o}C) (260X magnification)
(e) HAp-ZnO 20:2 (600 ^{o}C) (301X magnification)
(f) HAp-ZnO 20:2 (800 ^{o}C) (203X magnification)
(g) HAp-ZnO 20:2 (1000 ^{o}C) (147X magnification)

Energy Dispersive X-Ray Fluorescence (EDXRF) Analysis of HAp-ZnO Nanocomposites

Relative abundances of elemental oxides in HAp-ZnO nanocomposites are shown in Figure 5 and the corresponding data are presented in Table 3. It was observed that the concentrations of CaO, P_2O_5 and ZnO were the highest percentages (in order of decreasing content) in each composites. Other metal oxides were also found in minute amounts in all prepared composites. The amount of ZnO increased in the composites with increase in amount of ZnO nanoparticles added in HAp-ZnO nanocomposites.

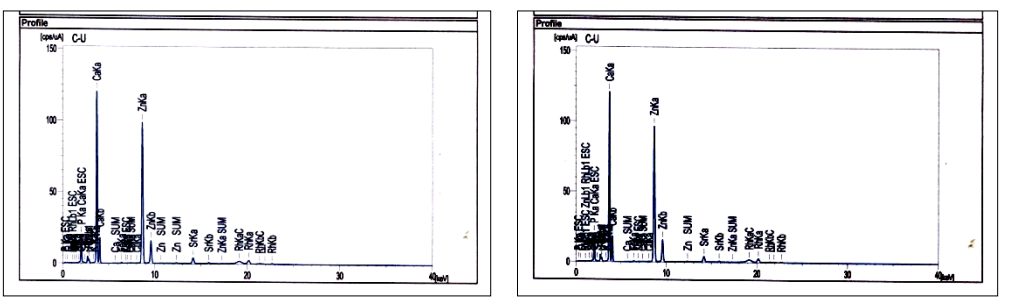

(a) (b)

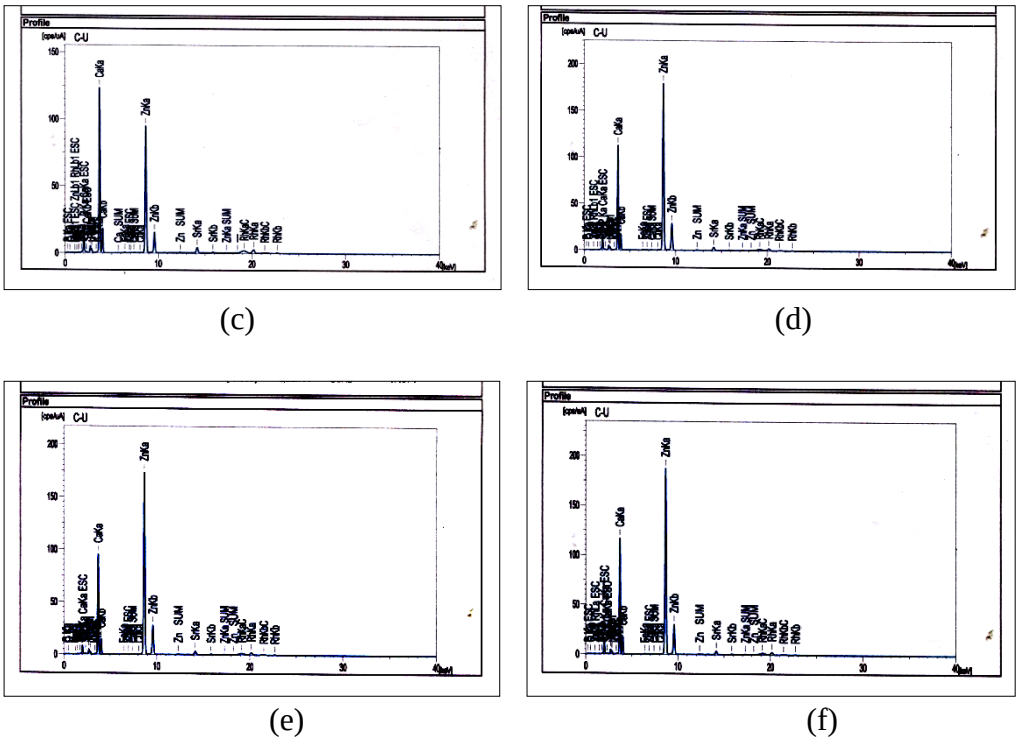

Figure 5: EDXRF spectra of HAp-ZnO (20:1) calcined at (a) 600ºC (b) 800 ºC (c) 1000 ºC and HAp-ZnO (20:2) calcined at (d) 600 ºC (e) 800 ºC and (f) 1000 ºC

Table 3: Relative Abundances of Elemental Oxide in HAp-ZnO Composites

Sample	Elemental oxide (%)										
	CaO	**P_2O_5**	**ZnO**	**MgO**	**SiO_2**	**Al_2O_3**	**SO_3**	**K_2O**	**SrO**	**Fe_2O_3**	**CuO**
1	50.370	34.473	5.884	2.985	2.593	2.505	0.660	0.294	0.151	0.077	0.009
2	51.882	35.166	5.977	-	2.565	3.071	0.798	0.299	0.155	0.077	0.010
3	50.337	34.510	5.500	2.782	2.741	3.091	0.534	0.276	0.147	0.073	0.009
4	49.555	32.343	11.622	-	2.280	2.936	0.730	0.297	0.157	0.066	0.014
5	53.949	31.766	13.634	-	-	-	-	0.376	0.185	0.073	0.018
6	50.865	31.107	12.246	-	2.354	2.486	0.401	0.298	0.168	0.060	0.015

1 = HAp - ZnO (20:1) at 600 ºC
2 = HAp - ZnO (20:1) at 800 ºC
3 = HAp - ZnO (20:1) at 1000 ºC
4 = HAp - ZnO (20:2) at 600 ºC
5 = HAp - ZnO (20:2) at 800 ºC
6 = HAp - ZnO (20:2) at 1000 ºC

Physical Properties of HAp, ZnO and HAp-ZnO Nanocomposites

pH of the HAp calcined at 900 ^{o}C was found to have 9.8. After incorporation of ZnO nanoparticles the pH values slightly decreased in the range of 9.3 to 9.6. However, addition of increase amount of ZnO did not appreciably change the pH value (Table 4).

Bulk density of HAp sample was 1.56 g mL^{-1}. The bulk density also slightly increased in HAp-ZnO nanocomposites compared to HAp sample. The bulk densities of the HAp-ZnO nanocomposites were in the range of 1.61 to 1.79 g mL^{-1}. It was found that among the nanocomposite samples, the porosity percent slightly decreased with increasing both temperature and amount of ZnO.

Table 4: Physical Properties of the Prepared Hydroxyapatite and Hydroxyapatite- Zinc Oxide Nanocomposites Calcined at Different Temperatures

No		Samples						
		HAp	HAp-ZnO (20:1)			HAp-ZnO (20:2)		
		900 ^{o}C	600 ^{o}C	800 ^{o}C	1000 ^{o}C	600 ^{o}C	800 ^{o}C	1000 ^{o}C
1	pH	9.8	9.5	9.3	9.6	9.4	9.3	9.5
2	Bulk density (g/mL)	1.56	1.59	1.61	1.61	1.61	1.70	1.72
3	Porosity (%)	18.32	9.60	9.30	6.94	7.53	5.85	5.56

Cytotoxicity Test of Prepared HAp and HAp-ZnO Nanocomposites

The cytotoxicity of HAp and HAp–ZnO nanocomposites were evaluated by brine shrimp cytotoxicity bioassay. The cytotoxicity of HAp and HAp-ZnO composites was expressed in terms of mean ± SEM (standard error mean) and LD_{50} (50 % Lethality Dose) and the results are shown in Table 5. In this experiment, standard potassium dichromate ($K_2Cr_2O_7$) was chosen because $K_2Cr_2O_7$ has well-known toxicity in this assay. The LD_{50} values of HAp sample, HAp-ZnO composites with two different ratios of 20:1 and

20:2 calcined at 1000 ^{o}C were found to be >1000 µg/mL. The LD_{50} values of standard $K_2Cr_2O_7$ was found to be 13.79 µg/mL.

According to Meyer's toxicity index, the sample with LD_{50} < 1000 µg/mL are considered as toxic, while the sample with LD_{50} > 1000 µg/mL are considered as non-toxic (Meyer *et al*., 1982). So HAp and HAp-ZnO composites prepared in this work showed no cytotoxic effect.

Table 5: Cytotoxicity of HAp Sample, HAp-ZnO Composites with Two Different Ratios of 20:1 and 20:2 Calcined at 1000 ^{o}C against *Artemia salina* (Brine Shrimp)

Samples	Percentages of Dead Brine Shrimp (Mean ± SEM) in Various Concentrations (µg/mL) of Samples					LD_{50} (µg/mL)
	0.1	1	10	100	1000	
HAp	0	0	0	0	3.33±5.77	> 1000
HAp-ZnO (20:1)	0	0	0	3.33±5.77	3.33±5.57	> 1000
HAp-ZnO (20:2)	0	0	0	3.33±5.77	3.333±5.57	> 1000
$K_2Cr_2O_7$*	3.33± 5.57	6.67 ± 5.77	20.00± 0.00	100.00 ± 0.00	100.00 ± 0.00	13.79

* Used as Cytotoxic Standard

Radiological Results of Skull Bone Defects Filled with HAp and HAp-ZnO Nanocomposites

After 14 days of operation incomplete skull bone defects were observed in the Wistar rat filled with HAp and control. On the other hand, bony defect was still observed in Wistar rat filled with HAp-ZnO (20:1) nanocomposites calcined at 1000 ^{o}C. However, a tiny bone defect remained in Wistar rat filled with HAp-ZnO (20:2) nanocomposites (Figure 6). After 30 days of operation, bony defect remained in the control whereas a tiny hole bone defect was observed in Wistar rat filled with HAp (Figure 7). Furthermore, in Wistar rat filled with HAp-ZnO nanocomposites (20:1) there was very little pointed bony defect remained. Complete bone healing was

observed by using HAp-ZnO (20:2). The composites bridge the defect and new bone was formed.

According to X-ray visions, it has some differences among different composite applications. HAp-ZnO composite defect bone applications showed better than other two X-ray visions.

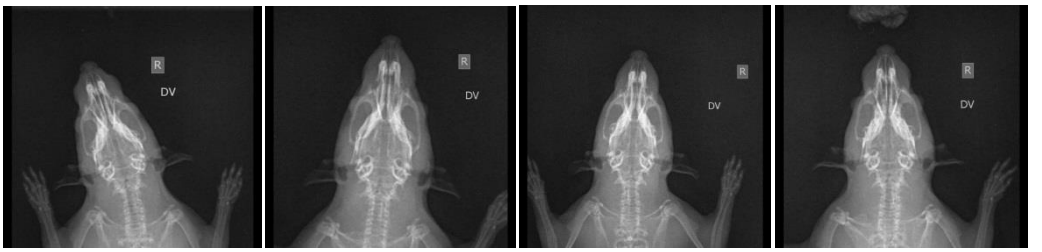

(a) (b) (c) (d)

Figure 6: 14 days Progressiveness of Bone Defect Healing in X-ray Diagnosis (a) Control (b) HAp at 900 ^{o}C (c) HAp-ZnO (20:1) calcined at 1000 °C

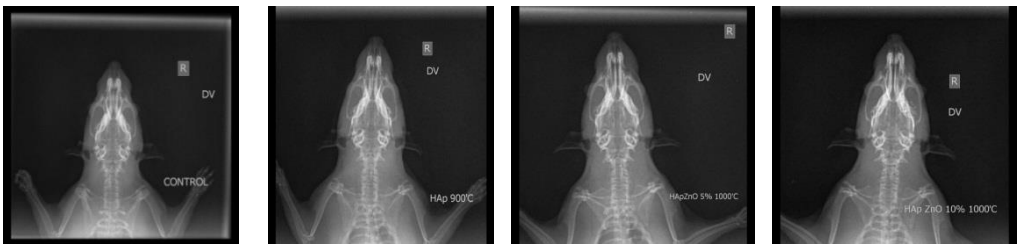

(a) (b) (c) (d)

Figure 7: 30 days Progressiveness of Bone Defect Healing in X-ray Diagnosis (a) Control (b) HAp at 900 ^{o}C (c) HAp-ZnO (20:1) calcined at 1000 °C (d) HAp-ZnO (20:2) calcined at 1000 °C

Histological Results of Skull Bone Defects Filled with HAp and HAp-ZnO Nanocomposites

At 14 days after the surgery, histology of fracture skull bone revealed that connective tissue was occupied especially fibroblast and admixed with net work of delicate bone trabeculae lined with osteoblast and formed from inner surface of wall of skull bone. Blood clot remnants were observed. Non-union

of skull bone was resulted (Figure 8a). Fracture site was filled with fibroblast and blood clots. Net work of delicate bone trabeculae lined with osteoblast and formed from inner surface of wall of skull bone. Incomplete cartilage union was found (Figure 8b). Coagulum (blood clot) was reduced in size and observed woven bone formation composed of few osteoblast and increased amount of chondrocytes. Complete with cartilage union was observed (Figure 8c). A few coagulum was found and mixed with few fibroblast. Woven formation was noted and accompanied with increased osteoblast and chondrocytes. A fracture site was replaced by few amount of trabecular bone. Predominantly cartilage with some trabecular bone was detected (Figure 8d).

The histological findings at 30 days showed that new trabecular bone formation was started from fracture site and composed of osteoblast and increased amount of chondrocytes. Predominantly cartilage with some trabecular bone was seen (Figure 9a). Trabecular bone formation was well organized and absence of blood clots and fibroblast was observed. Osteoblast was seen in inner layer of fracture bone. Chondrocytes are filled in some trabecular bone areas. Incomplete bony union with intermediate ossification was observed. Equal amounts of cartilage and trabecular bone was detected (Figure 9b). There was increased amount of osteocytes in centre area of bony fracture site. Chondrocytes were filled in some trabecular bone areas. Incomplete bony union with late ossification was detected. Predominantly trabecular bone with some cartilage was observed (Figure 9c). There was complete new formation of trabecular bone in fracture site. Complete union of fracture area was observed in entire bony fracture site. Complete union of fracture bone was resulted (Figure 9d).

Due to histological findings, HAp-ZnO composite with ratio of 20:2 at 1000 °C group was the best with good scoring within 30 days after application.

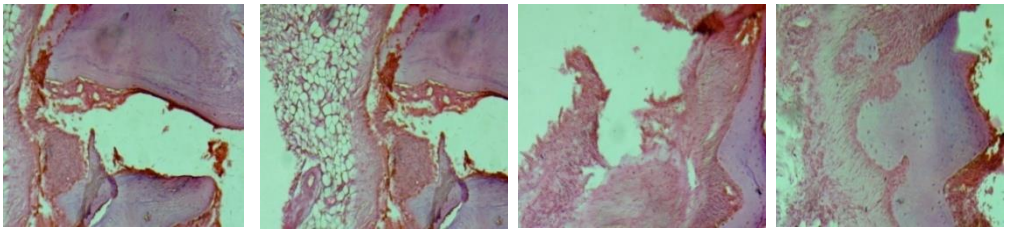

(a) (b) (c) (d)

Figure 8: Photomicrographs of histopathology of 14 days bony healing with (a) Control (b) HAp calcined at 900 ºC (c) HAp : ZnO (20 : 1) calcined at 1000 ºC (d) HAp : ZnO (20 : 2) at 1000 ºC

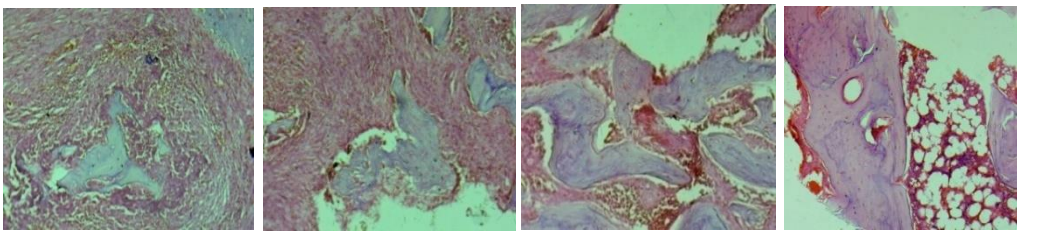

(a) (b) (c) (d)

Figure 9: Photomicrographs of histopathology of 30 days bony healing with (a) Control (b) HAp calcined at 900 ºC (c) HAp : ZnO (20 : 1) calcined at 1000 ºC (d) HAp : ZnO (20 : 2) at 1000 ºC

Conclusion

HAp-ZnO nanocomposites were successfully prepared by incorporation of ZnO nanoparticles to HAp derived from waste goat bone calcined at 900^{o}C with the ratio of 20:1 and 20:2. After incorporation of ZnO to HAp with the ratios of 20:1 and 20:2, the characteristic peaks of both HAp and ZnO were found in the X-ray diffractograms of HAp-ZnO nanocomposites. The crystallite sizes were in the range of 40.28 nm to 49.10 nm and found to increase with increase in temperature and with increase in amount of ZnO. The shifts in peak positions and the change of lattice constant of HAp after incorporation of ZnO nanoparticles indicated the substitution of Zn ion in Ca ion. FT IR spectral data revealed the characteristic

absorption peaks of PO_4^{3-}, OH^- and ZnO. The absorption peaks of ZnO shifted from 418 cm^{-1} to higher wavenumbers (437 to 474 cm^{-1}) in HAp-ZnO nanocomposites. HAp-ZnO nanocomposites showed elongated crystalline structures in SEM analysis. EDXRF spectra showed the highest content of CaO,P_2O_5 and ZnO in these nanocomposites.

Brine shrimp cytotoxicity bioassay indicated that HAp and HAp-ZnO nanocomposites were not cytotoxic. Orthopedic application of HAp and HAp-ZnO nanocomposites as filling material were conducted on Wistar rats. After 30 days implantation, the newly formed bone tissue appeared within the bone defect in the Wistar rat. X-ray diagnosis and histological findings confirmed the successful filling of the prepared samples. Thus, HAp-ZnO nanocomposites have the potential to improve numerous orthopedic and dental applications.

Acknowledgements

The authors would like to thank the Myanmar Academy of Art and Science for allowing to present this paper and Professor and Head Dr Tin Tin Mya, Department of Chemistry, Mandalar Degree College for her kind encouragement.

References

Anita, S., Ramachandran, T., Koushik, C.V., Rajendran, R. and Mahalakshmi, M. (2010). "Preparation and Characterization of Zinc Oxide Nanoparticles and A Study of the Anti-microbial Property of Cotton Fabric Treated with the Particles". *JIATM*, vol.6 (4), pp.1-6.

Deepa, C., Begum, A. N. and Aravindan, S. (2013). "Preparation and Antimicrobial Observations of Zinc Doped Nanohydoxyapatite". *Nanosystems: Physics, Chemistry, Mathematics,*vol.4 (3), pp. 370-377.

Figueiredo,M., Fernando, A., Martins, G., Freitas, J., Judas, F. and Figueiredo, H. (2010). "Effect of Calcination Temperature on the Composition and Microstructure of Hydroxyapatite Derived from Human and Animal Bones". *Ceramics International*,vol.36, pp. 2383-2393.

Kini, U. and Nandeesh, B. N. (2012). Physiology of Bone Formation, Remodeling and Metabolism. In *Radionuclide and Hybrid Bone Imaging*. (Eds.) Foggelman, I., Gnanasegaran, G. and Wall , H. Berlin: Springer, pp. 29-57.

Meyer, B.N., Ferrigni, N.R., Putnam, J.E., Jacobsen, L.B., Nichols, D.E. and McLaughlin, J.L. (1982). "Brine Shrimp: A Convenient General Bioassay for Active Plant Constituents". *Planta Medica*, vol.45**,** pp. 31-34

Moldovan, M., Prodan, D., Popescu, V., Prejmerean, C., Sarosi, C., Saplonț ai, M., Tă lu, S. and Vasile,E. (2015). "Structural and Morphological Properties of HA-ZnO Powders Prepared for Biomaterial". *Open Chem.,* vol.13, pp. 725–733.

Nawaz, H. R., Solangi, B.A., Zehra, B. and Nadeem, U. (2011). "Preparation of Nano Zinc Oxide and its Application in Leather as Retaining and Antibacterial Agent". *Canadian Journal on Scientific and Industrial Research*,vol.2(4), pp. 165-170

Okada, M. and Matsumoto, T. (2015). "Synthesis and Modification of Apatite Nanoparticles for Use in Dental and Medical Applications". *Japanese Dental Science Review*, vol.51, pp.85-95

Singh, A., Kumar, R., Malhotra, N. and Suman. (2012). "Preparation of ZnO Nanoparticles by Solvothermal Process". *International Journal for Science and Emerging Technologies with Latest Trends*,vol.4(1), pp.49-53

Sverdrup, H.U., Johnson, M.W. and Fleming, R.H. (1942). "*The Oceans Their Physics, Chemistry and General Biology*". New York: Prentice-Hall, Inc., p. 186

Vanaja, A. and Rao, K. S.. (2016). "Precursors and Medium Effect on Zinc Oxide Nanoparticles Synthesized by Sol-Gel Process". *International Journal of Applied and Natural Sciences,* vol. 5(1), pp. 53-62

Yadav, A., Prasad, V., Kathe, A. A., Raj, S., Yadav, D., Sundaramoorthy, C. and Vignesharan, N. (2006). "Functional Finishing in Cotton Fabric using Zinc Oxide Nanoparticles". *Bull Matter Sci*, vol.29(6), pp. 641-645

Ylinen, P. (2006). *Applications of Coralline Hydroxyapatite with Bioabsorbable Containment and Reinforcement as Bone Graft Substitute*. Helsinki: Academic Dissertation, University of Helsinki

Zak, A. K., Majid, W.H.A., Mahmoudian, M. R., Darroudiand, M. and Yousefi, R. (2013). "Starch-stabilized Synthesis of ZnO Nanopowders at Low Temperature and Optical Properties Study". *Advanced Powder Technology,* vol.24, pp.618-624

Zhou, H. and Lee, J. (2011). "Nanoscale Hydroxyapatite Particles for Bone Tissue Engineering". *Acta Biomater***,** vol.7(7), pp.2769- 2781